Post Processing of Laser Scanner Measurements for Testing Advanced Driver Assistance Systems

Jan Erik Stellet[1)], Leopold Walkling[2), formerly 1)], J. Marius Zöllner[3)]
[1)]Robert Bosch GmbH, Corporate Research, Vehicle Safety and Assistance Systems, 71272 Renningen, Germany
[2)]BMW Group, 80788 Munich, Germany
[3)]Research Center for Information Technology (FZI), 76131 Karlsruhe, Germany

***Abstract*—Testing of advanced driver assistance systems demands a highly accurate representation of the vehicle's environment, e.g. obtained by laser scanner sensors. In contrast to typical on-line assistance functions, the purpose of generating reference data allows full batch processing of the raw sensor measurements. Therefore, object tracking algorithms can make use of both past and future measurement information. Hence, ambiguities during object detection and data association may be resolved in a principled manner.**

Although many works consider the tracking of vehicles using LIDAR[1] sensors, the specifics of batch processing have not been investigated yet. This paper proposes novel non-causal approaches to detecting and tracking vehicles in 2-D scan point clouds given by an automotive LIDAR sensor. Evaluations based on experimental data show how post processing can improve the trade-off between the suppression of clutter measurements and prompt detection as well as the estimation accuracy.

I. Introduction

Intelligent vehicles, i.e. characterised by advanced driver assistance functions with environment perception, constitute an important field of applied sensor data fusion. To objectively test a perception system, ground truth information is required, as discussed in our previous work [1]. The same holds for the data-driven generation of simulation scenarios, e.g. in order to evaluate algorithms for behaviour planning of automated vehicles [2], [3]. Due to a fairly high spatial and temporal resolution, LIDAR sensors are frequently used to obtain such reference data [4], [5].

Laser scanner sensors obtain a sparse depth image of the environment. Each depth value corresponds to one reflection *(scan point)* of a laser beam. In this work, 2-D LIDAR sensors with a narrow vertical opening angle are considered. They perceive a planar depth image of the environment as shown in Fig. 1. However, scan points lack spatial and temporal associations as well as motion information. Therefore, the goal is to cluster reflections belonging to individual objects, to associate the measurements over time and to estimate unobservable motion states. This yields *object tracks* with motion information.

In principle, reference data may be obtained using real-time capable algorithms, which have been developed in order to realise driver assistance functions, see e.g. [6]–[8]. However, in contrast to this purpose, reference data can be generated batch-wise which removes several crucial restrictions of on-line processing. Thus, this work investigates the benefits of post processing of LIDAR data where both past and future measurements are available. More specifically, two aspects will be addressed with the following **contributions**:

- Initialising new object tracks requires a trade-off between suppression of clutter measurements and prompt recognition of relevant objects. In an off-line processing approach, this compromise can be improved by backward propagation of information. Therefore, a forward-backward object tracking algorithm (Sec. III-C–III-E) is developed. The method uses a LIDAR-specific quality metric (Sec. III-B) in order to find accurate initial values which minimise the risk of an early track loss.
- Real-time constraints and computational limitations, e.g. on embedded devices, complicate the handling of raw scan point measurements. Instead, derived representations, e.g. parametric contour models, are often used. We will employ a model-free alternative method for associating scan points to object tracks based on a consistent motion criterion (Sec. III-D). This criterion minimises the dependence of the tracking algorithm on correct a-priori clustering of scan points.

The advantages of the proposed methods over a baseline, on-line capable algorithm are evaluated with experimental data in

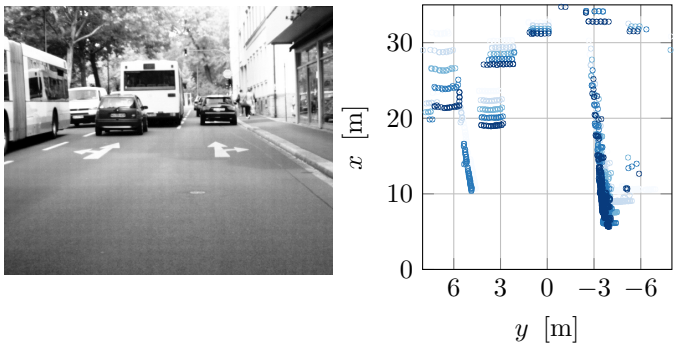

Fig. 1: Exemplary LIDAR measurements from an urban road with three lanes. The image shows how the scan point measurements evolve over a period of 1 s, from light to dark colour. Reflections of the laser rays at the rear or front of other vehicles manifest as lines or characteristic L-shapes.

[1]**L**ight **D**etection **a**nd **R**anging.

terms of state estimation accuracy and track length (Sec. IV).

The **organisation** of the remainder of this paper is as follows: Background information and related works are first introduced in Sec. II. Subsequently, the developed approaches to off-line processing are detailed in Sec. III. Evaluation results follow in Sec. IV. A summary and discussion of possible further extensions in Sec. V concludes this paper.

II. Background on laser scanner signal processing and related work

The objective of LIDAR signal processing is to obtain a compact and information rich environment representation from raw scan point clouds. In an automotive context, the position and motion of other road users, e.g. vehicles, are of high relevance and will be in the focus of this work. This is usually achieved by three algorithmic steps as visualised in Fig. 2:

1) Extended objects are usually represented by multiple scan points, especially at short distances. Thus, scan points which belong to the same object must be grouped into *segments*. This segmentation is often based on the local neighbourhood of scan points that is measured with distance measures [6], [7].
2) A *track* is established from measurements of the same object from multiple time steps. Various methods exist for associating the measurements over time, depending on the targeted objects, their environment, and the sensor's measurement principle [7], [9], [11]. The decision to initialise a new track with scan points that cannot be assigned to one of the previously observed tracks is based on relevance criteria. Measurements of a vehicle may be distinguished from clutter if they show a distinct shape [6] or a consistent motion [8].
3) In order to estimate the motion state of a track, a single reference point is calculated from the associated scan points, e.g. a point cloud's centroid [6]. More sophisticated approaches avoid pseudo motions of this reference point caused by a non-stationary point cloud, e.g. due to dynamic occlusions [12]. Given the temporal sequence of reference point measurements, a state estimator, e.g. an Extended Kalman filter (EKF)[2] [11], can be employed to infer unobservable motion state variables of a dynamic motion model [13], such as velocities and accelerations.

We remark that a successful track extension depends on the accuracy of the motion state estimate. That is because the predicted locations of a track's current scan points are usually used as a search region for associating scan points from a new time step.

For real-time applications, the above steps can only make use of past LIDAR scans. Post processing of an entire sequence of scans on the other hand offers additional flexibility which will be leveraged in the following. To the best of the authors' knowledge, no detailed evaluations of such approaches have yet been published apart from a sketch of the idea given in [2]. Nevertheless, sound theoretical foundations of reconstructing dynamic object tracks from collected measurement data have been developed both for estimating the state of a single target [14] and multiple target tracking [15].

[2]Instead of an EKF, other implementations of a Bayes filter for non-linear system models, e.g. the Unscented Kalman filter, may be used. Investigating the differences between such methods [10] lies out of this work's scope.

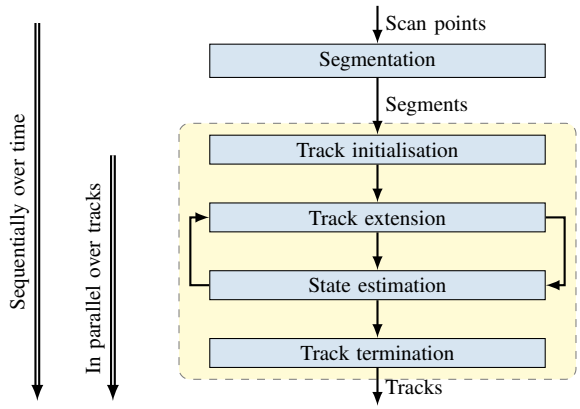

Fig. 2: In on-line applications, measurements are processed strictly sequentially over time: After segmenting the laser scan points, object tracks are extended, terminated or newly initialised.

III. Approaches to off-line signal processing

The steps of our approach are explained in roughly the same order in which they are applied to the observations of a single object, see Fig. 3. We start with a high level description of the proposed algorithm in Sec. III-A. Then, in Sec. III-B we explain how we rate segments of scan points for their observability. Subsequently, the initialisation of a track is detailed in Sec. III-C. We provide further details on how tracks are extended to new time steps in Sec. III-D, as well as on how their start and end are determined. Finally, we describe our approach to state estimation in Sec. III-E.

A. Overview

On-line tacking algorithms try to detect objects as early as possible, but detection always involves selecting a threshold that determines the trade-off between early detection and few false positives. In off-line tracking, this dilemma can be relaxed: Detection merely needs to ensure that every object is detected in at least one time step.

First, the goal is to initialise a track for an object at a time when this object is easy to observe, thus making the initial state estimates more reliable. To this end, we introduce a quality index for segments (Sec. III-B) which is independently calculated for all segments from every time step. We refer to the set of segments and corresponding quality indices as the *register*. Note that initially, the register contains more than one segment corresponding to the same object, if it has been observed in multiple time steps. These redundant entries will be removed when their constituent scan points are associated to a track.

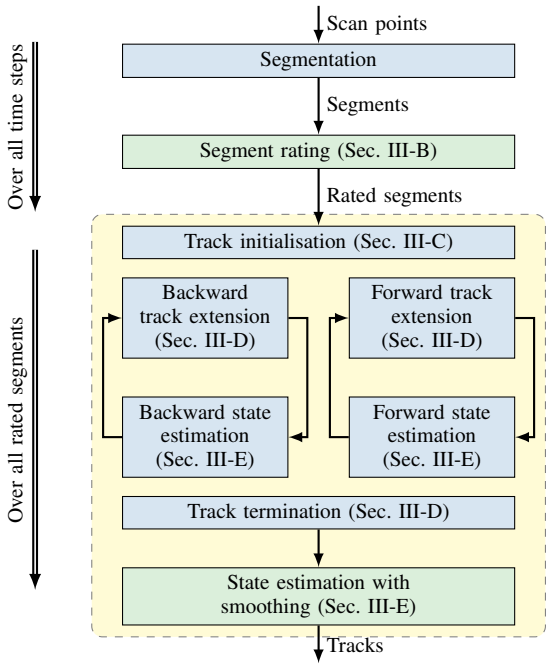

Fig. 3: A key principle of the proposed off-line approach is to defer the decision for a track initialisation until sufficient evidence is available. To this end, a quality rating for scan point segments is introduced. A track is initialised for the best-rated segments and subsequently extended in forward and backward direction. State estimates are obtained by a forward filtering pass and additional backward smoothing.

We now initialise a track starting with the segment that features the highest overall quality index, see Sec. III-C for details. Next, we extend the active track to a new time step by associating new scan points and updating the motion state estimate. The association of scan points is solved using the Weighted Iterative Closest Point (WICP) algorithm as detailed in Sec. III-D. Iteratively, the current track is extended into the past and the future as seen from the initial time step, until a stopping criterion is met. Upon completion, the active track is stored and its corresponding scan points as well as segments are precluded from the generation of further tracks. Given all scan points associated to this track, the object's motion state is finally estimated by an Extended Rauch-Tung-Striebel smoother (EKS) algorithm, see Sec. III-E.

We repeat the above steps, each time taking the remaining segment with the highest quality measure from the updated register, until no entry remains. Therefore, we repeatedly perform single object tracking both forward and backward in time, each time taking the object that is best visible.

B. Segment rating

The quality index determines the order of track initialisation attempts. Conceptually, this measure rates how reliably an object can be observed at a certain time. It is calculated for a segment of scan points $\mathcal{M}$ as follows:

$$J(\mathcal{M}) \coloneqq w_1 \, J_{\text{cardinality}}(\mathcal{M}) + w_2 \, J_{\text{shape}}(\mathcal{M}) \ . \quad (1)$$

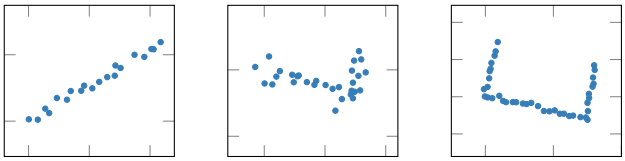

(a) I-shape (b) L-shape (c) U-shape

Fig. 4: Relevant objects, i.e. vehicles, are approximately cuboidal. Depending on the pose relative to the sensor, this leads to typical point configurations in the 2-D laser scans. The goodness of fit is included in the quality rating of segments from Sec. III-B.

The weights w_1 and w_2 are design parameters. The first term, $J_{\text{cardinality}}(\mathcal{M})$, is a sigmoid function of the number $|\mathcal{M}|$ of scan points in segment $\mathcal{M}$

$$J_{\text{cardinality}}(\mathcal{M}) = \frac{1}{1 + \exp\left(-\alpha \left(|\mathcal{M}| - N_{\text{ref}}\right)\right)} \ , \quad (2)$$

where α and N_{ref} are design parameters. We include this term to reward segments with a high number of scan points which correlates with low distance, large size, and good reflectivity for laser beams.

The second term J_{shape} is based on a shape recognition approach for vehicles from LIDAR sensors, as proposed in [6], see also [16] for a recent analytical approach. In this approach, the segment to be analysed is compared to L-, I-, and U-shapes as illustrated in Fig. 4. By applying a threshold to the residual distance between scan points and the fitted model shape, we determine the number of scan points $N_{\text{inlier}}(\mathcal{M})$ that support the model, i.e. the inliers. Thus, we can measure the quality of the current segment in terms of model fit as

$$J_{\text{shape}}(\mathcal{M}) = \frac{N_{\text{inlier}}(\mathcal{M})}{|\mathcal{M}|} \ . \quad (3)$$

C. Track initialisation

By allowing free choice of when to initialise a track, this point in time can be chosen in such a way, that estimating the state becomes more reliable, thus decreasing the likelihood of incorrect data association. Therefore, track initialisation starts with the segment which currently has the highest quality index. Assuming that this segment corresponds to a real object, this segment is guaranteed to be the best observation of the object, with regard to the quality index.

An initial motion state estimate, which is needed for further track extensions and state estimation, is then generated. We are particularly interested in an initial velocity estimate since scan point measurements do not carry motion information. To this end, we consider all segments from the time steps immediately next to the detection time t_0, i.e. t_{-1} and t_1. This situation is illustrated in Fig. 5. Following a Multi-Hypothesis Tracking scheme, we generate several motion state hypotheses based on

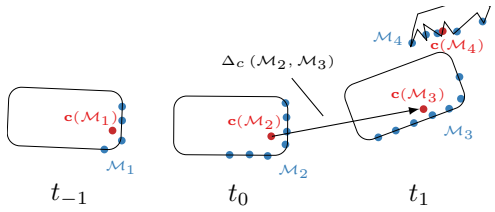

Fig. 5: Illustration of the situation at track initialisation: Three time steps t_{-1}, t_0, t_1 are considered, but there may be more than one segment in a time step, e.g. due to clutter as at t_1.

a Constant Velocity (CV) model, given by the following set of velocity estimates:

$$\begin{aligned}\big\{\Delta\mathbf{c}_{i,k}\colon &\|\Delta_c(\mathcal{M}_i,\mathcal{M}_j)\| < \theta_\mathrm{d}, \|\Delta_c(\mathcal{M}_j,\mathcal{M}_k)\| < \theta_\mathrm{d},\\ &\|\Delta_c(\mathcal{M}_j,\mathcal{M}_k) - \Delta_c(\mathcal{M}_i,\mathcal{M}_j)\| < \theta_{\Delta\mathrm{v}},\\ &D(\mathcal{M}_i,\mathcal{M}_j) < \theta_\mathrm{D},\ D(\mathcal{M}_j,\mathcal{M}_k) < \theta_\mathrm{D}\big\}\end{aligned} \tag{4}$$

$$\begin{aligned}\text{with } &\Delta_c(\mathcal{M}_i,\mathcal{M}_j) \coloneqq \mathbf{c}(\mathcal{M}_i) - \mathbf{c}(\mathcal{M}_j),\\ &i \in \mathcal{I}_{t_{-1}}, k \in \mathcal{I}_{t_1}.\end{aligned}$$

Here, $\mathbf{c}(\mathcal{M})$ is the centroid of the scan points in segment $\mathcal{M}$, j is the index of the segment chosen for track initialisation and $\mathcal{I}_{t_{-1}}$ and $\mathcal{I}_{t_1}$ denote the sets of the indices of all segments from the time steps $\{t_{-1}, t_1\}$. The Procrustes distance $D(\mathcal{M}_i,\mathcal{M}_j)$ between segment $\mathcal{M}_i$ and segment $\mathcal{M}_j$ is a measure for the dissimilarity of the two point clouds [17]. The generation of motion state hypotheses is governed by the threshold parameters $\theta_{(\cdot)}$.

For each motion state hypothesis, we perform the tracking procedure (Sec. III-D, Sec. III-E) independently of the other hypotheses. When completed, only the longest track and its scan point associations are kept.

D. Track extension and termination

In this section we describe how we associate scan points from a new time step with the active track. The new scan points provide a measurement of the object's position and will be used to update the estimates of the object's kinematic state.

The most recent point cloud is first predicted to the next time step based on the motion model and the latest state estimate. To reduce the number of scan points from the new time step that are to be considered in the following, a gating criterion on the distance to the predicted scan points is applied.

Then, the WICP algorithm is used to align the predicted point cloud with scan points within the gate. This yields the associations of each observed scan point to a point from the prediction. However, the WICP algorithm associates only scan points which are close to the points from the object's predicted point cloud. To allow the object's appearance to grow by previously occluded edges, we perform an additional clustering step, using the already associated scan points as seeds. A reference point which is used to update the state estimate in the EKF is then calculated from the combined set of associated and additionally clustered scan points.

We want to repeat track extensions only for as long as the object is visible. Hence, we need to detect an object's disappearance which is checked using three criteria. First, we compute the Procrustes distance [17] between the predicted and observed point cloud and compare it with a fixed threshold. As a second criterion, we check the consistency of the estimated motion, by calculating from our state estimate the likelihood of observing the resulting motion, given all previous motion states. Third, we compare the number of associated scan points to a minimum threshold. A track is discontinued if the termination criteria above are fulfilled for at least K_term adjacent time steps.

E. Joint state estimation of forward and backward pass

As has been mentioned in the previous section, the extension of a track to a new time step relies on an estimate of the current motion state. We will discuss our approach to motion state estimation in the following, taking into account that tracks are simultaneously extended both forward and backward in time.

We employ the non-linear Constant Turn Rate and Acceleration (CTRA) kinematic motion model which features the state $\mathbf{x} := \begin{bmatrix} x & y & v & \theta & a & \omega \end{bmatrix}^\top$ where v is the target's velocity, θ the heading angle, a acceleration and ω the yaw rate. The motion dynamics are defined by the following differential equation [13]:

$$\begin{bmatrix}\dot{x}(t)\\ \dot{y}(t)\\ \dot{v}(t)\\ \dot{\theta}(t)\\ \dot{a}(t)\\ \dot{\omega}(t)\end{bmatrix} = \begin{bmatrix}v(t)\cos(\theta(t))\\ v(t)\sin(\theta(t))\\ a(t)\\ \omega(t)\\ 0\\ 0\end{bmatrix} + \begin{bmatrix}0\\0\\0\\0\\w_a(t)\\w_\omega(t)\end{bmatrix}. \tag{5}$$

Here, w_a and w_ω denote Gaussian white noise processes with time-invariant power spectral densities S_a and S_ω, respectively. Note that the system model equations in discrete time differ between forward and backward direction. They are derived from (5) by integration [18].

According to Sec. III-C, a track is initialised at a time t_0 with a tentative state expectation $\mathbf{x}_0^-$ and covariance $\mathbf{P}_0^-$. Each successful track extension to a time t_k yields a measurement $\mathbf{y}_k$ that relates to $\mathbf{x}_k$ through a (non-) linear measurement model $\mathbf{y}_k = \mathbf{h}(\mathbf{x}_k, \mathbf{v}_k)$ where $\mathbf{v}_k$ is assumed as Gaussian noise $\mathbf{v}_k \sim \mathcal{N}(\mathbf{0}, \mathbf{R})$.

Therefore, the goal is to infer an estimate of the state distribution $p(\mathbf{x})$ at $t_1, \ldots, t_k$ and $t_0, t_{-1}, \ldots, t_{-l}$ from the measurements $\mathbf{y}_{0:k} \coloneqq \mathbf{y}_0, \mathbf{y}_1, \ldots, \mathbf{y}_k$ and $\mathbf{y}_{0:-l} \coloneqq \mathbf{y}_0, \mathbf{y}_{-1}, \ldots, \mathbf{y}_{-l}$ in forward and backward direction, respectively. We assume a Gaussian distribution $\mathbf{x}_k \sim \mathcal{N}(\hat{\mathbf{x}}_k, \mathbf{\Sigma}_k)$ of the state although the scheme can be easily adapted to general distributions.

The simplest solution is to decompose the task into separate state estimation problems for the forward and backward direction and solve it using two independent estimators. However, this way we would ignore all observations from one pass when estimating the motion states of the other. Yet, especially in the first few steps of the tracking process, we want to minimise

uncertainty and thus make efficient use of all available measurement information.

Therefore, an approach has been developed that iteratively performs forward and backward track extension, as is illustrated in Fig. 6. State estimates at the track's boundaries are obtained from the full measurement information from both directions. The approach relies on a repetition of four steps, employing Bayesian *filtering* and *smoothing* [14] in alternate order:

1) Starting in the forward direction, an EKF yields an estimate $p(\mathbf{x}_k|\,\mathbf{y}_{0:k})$ for $k > 0$.
2) A first smoothing pass is implemented with an EKS which yields the refined estimates $p(\mathbf{x}_0, \ldots, \mathbf{x}_k|\,\mathbf{y}_{0:k})$. Observe that the estimate at t_0 now incorporates all future measurement information, thus replacing the tentative value $\mathbf{x}_0^-$. This refinement of the initial state reduces the linearisation errors in the EKF equations that would otherwise hinder a successful track extension in the opposite direction.
3) An estimate $p(\mathbf{x}_{-l}|\,\mathbf{y}_{0:-l})$ is obtained for $l > 0$ by applying an EKF to the backward state transition model as derived from (5). The initial state distribution $p(\mathbf{x}_0)$ follows from the second step.
4) Finally, a second smoothing pass yields $p(\mathbf{x}_{-l}, \ldots, \mathbf{x}_0|\,\mathbf{y}_{0:-l})$.

The approach is similar to the globally iterated linear filter-smoother [19], a variant of the EKF which also performs backward propagation of state estimates. By updating the estimate of $\mathbf{x}_0$ and repeating the linearisation with this more accurate estimate, it reduces errors from linearisation of significant system non-linearities.

At the start of this iterative scheme, we repeatedly update all available estimates, once a new measurement becomes available. Nevertheless, we do not expect further improvements of the initial state estimate after a few iterations. In order to minimise the computational effort, the extension of a track is thereafter performed independently in the forward and backward direction. These extension passes are continued until the track termination criterion is fulfilled in both directions.

Once the boundaries of the track are known, the final motion state estimate is obtained by a Kalman filtering and smoothing pass over all time steps in the forward direction. We remark that estimating the initial state from measurements and filtering these measurements again may lead to overconfident estimates. Thus, we initialise the state covariance with large values and rely on the mean state estimate primarily as a good initial guess to minimise linearisation errors.

IV. Evaluation Results

The experimental evaluation should reveal whether the proposed off-line processing scheme can improve the track quality. One aspect of track quality is the accuracy of the state estimates, which is assessed in Sec. IV-A. A second measure of track quality, analysed in Sec. IV-B, is the average track length [13].

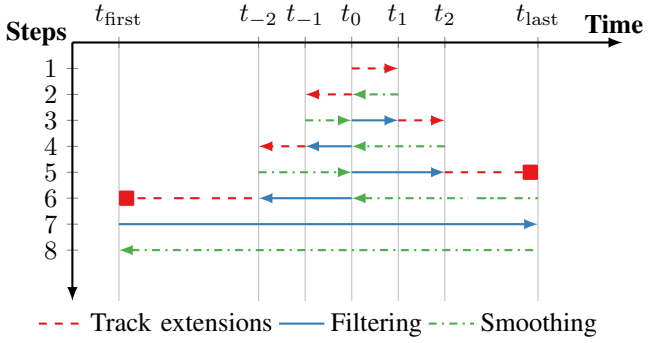

Fig. 6: Sequence of track extensions and state estimation updates: The first track extension steps (1–4) are performed in alternating direction. After this start-up phase, extension steps are performed individually in the forward and backward direction (5–6), until the track termination criterion is met. Lastly, the state is estimated by a final filtering and smoothing operation over the entire track (7–8).

In order to evaluate the advantages gained by off-line processing, an on-line capable algorithm according to Fig. 2 is used as a baseline. This implementation performs track extensions solely in the forward direction. Moreover, state estimates are obtained by an EKF whereas the off-line algorithm uses an additional smoothing pass. However, all remaining parts and criteria of the two implementations, e.g. the criteria for initialising and terminating a track, are the same. The rationale is that the evaluation should focus on the methodological differences between on-line and off-line processing.

A. State estimation accuracy

In order to quantitatively assess the accuracy of the motion state estimates, ground truth values are needed. Following the approach presented in [20], two experimental vehicles shown in Fig. 7 are equipped with a highly accurate self-localisation system based on differential GPS coupled with inertial measurement units[3]. The ego-vehicle, carrying a 2-D laser scanner with four beams[4], remains stationary at the origin of a ground-fixed Cartesian coordinate system. Ground truth values for the target vehicle's trajectory can be calculated from the global poses and compared to the estimates.

An accelerated approach and left turn across manoeuvre in front of the ego-vehicle is conducted on a closed test track. Thus, notable accelerations as well as rotations are included. This trajectory and the motion state are shown in Fig. 8. It can be seen that the accuracy of the state estimates is improved significantly by post processing, especially at the beginning of the track.

In order to quantitatively assess this difference, the experiment is repeated ten times. The sample mean $\mu_{\Delta(\cdot)}$ and sample standard deviation $s_{\Delta(\cdot)}$ are calculated for the errors $\Delta(\cdot)$ in

[3] *Automotive Dynamic Motion Analyzer (ADMA)* by GeneSys Elektronik GmbH.

[4] *ibeo LUX 2010* by Ibeo Automotive Systems GmbH.

TABLE I: Error statistics for ten turn across manoeuvres. With forward tracking and causal state estimation (top row), shorter tracks and higher standard deviations are obtained. The proposed algorithm with backward tracking and smoothing consistently achieves the highest accuracy. The additional smoothing step reduces the standard deviation by 15 % to 58 % compared to the filtered estimates (middle row).

Approach	No. of Cycles	v [m/s]		a [m/s^2]		ω [rad/s]	
		$\mu_{\Delta v}$	$s_{\Delta v}$	$\mu_{\Delta a}$	$s_{\Delta a}$	$\mu_{\Delta \omega}$	$s_{\Delta \omega}$
Baseline	523	−0.557	1.310	−0.038	1.21	0.050	0.128
New (filtered)	1212	−0.227	0.849	−0.003	0.767	0.021	0.095
New (smoothed)	1212	−0.312	0.723	−0.185	0.601	0.003	0.040

TABLE II: Statistics on tracks found in laser scanner recordings with a duration of 30 min per street type. On motorways, fewer and longer tracks are initiated due to the separation of the two traffic directions. Overall, the median track lengths can be increased by the backward tracking approach.

		Urban	Rural	Motorways
Number of all tracks	Baseline	2086	2375	1273
	New	2505	2727	1597
Number of tracks confirmed as vehicles	Baseline	319	222	150
	New	403	271	182
Number of common tracks	Baseline	286	178	129
	New	308	182	127
Median length of common tracks	Baseline	2.4 s	2.0 s	6.4 s
	New	3.1 s (+31.1 %)	2.5 s (25.0 %)	7.8 s (+20.5 %)

Fig. 7: Experimental vehicles for evaluating the state estimation accuracy. The laser scanner sensor is mounted at the front of the first vehicle. Both vehicles carry self-localisation units based on differential GPS and inertial measurements.

velocity v, acceleration a and yaw rate ω over all cycles. As an additional figure for comparison, the filtered state estimates of the new algorithm prior to the smoothing pass are included in the comparison. The results in Tab. I reveal that smoothing alone reduces the standard deviation of the estimates by 15 % to 58 %.

B. Track length

The purpose of the second experiment is to evaluate how much information is extracted from the raw LIDAR measurements in real traffic scenes. To this end, we analysed the number of generated tracks and their lengths. When comparing two algorithms on the same dataset, these figures indicate if tracks are initialised with a delay or terminated prematurely [21]. This is evaluated using recordings from three categories of street types – urban and rural roads as well as motorways – with a duration of 30 min each.

In order to reduce the effect of clutter on these figures, we restrict the evaluation to relevant objects. Here, the focus is on road users, e.g. cars or trucks, excluding static objects. Making this distinction can be achieved by a number of heuristics or machine learning techniques. Since the details of such approaches are not in the scope of this work, object classification is taken from a built-in routine of the employed LIDAR sensor. Only tracks which have been classified as vehicles are included in the evaluation. Moreover, the median track lengths are only compared for objects which are present in the results of both the baseline and the proposed algorithm. Note that multiple short tracks from one algorithm may be associated to one long track from the other algorithm.

Tab. II shows the statistics of the tracks per dataset. On average, 20 % to 31 % longer tracks are achieved by backwards track extension. The longest tracks are achieved on motorways where the road layout causes fewer occlusions than on narrow and curvy streets.

V. Conclusion

This work has proposed novel post processing methods for estimating vehicle motion tracks from laser scanner measurements. Despite the maturity and sophisticatedness of LIDAR data processing techniques for on-line driver assistance functions, it has not been investigated in depth so far, how off-line processing can enhance the estimation accuracy.

It is the authors' belief that having accurate reference measurements will play an important role in the development

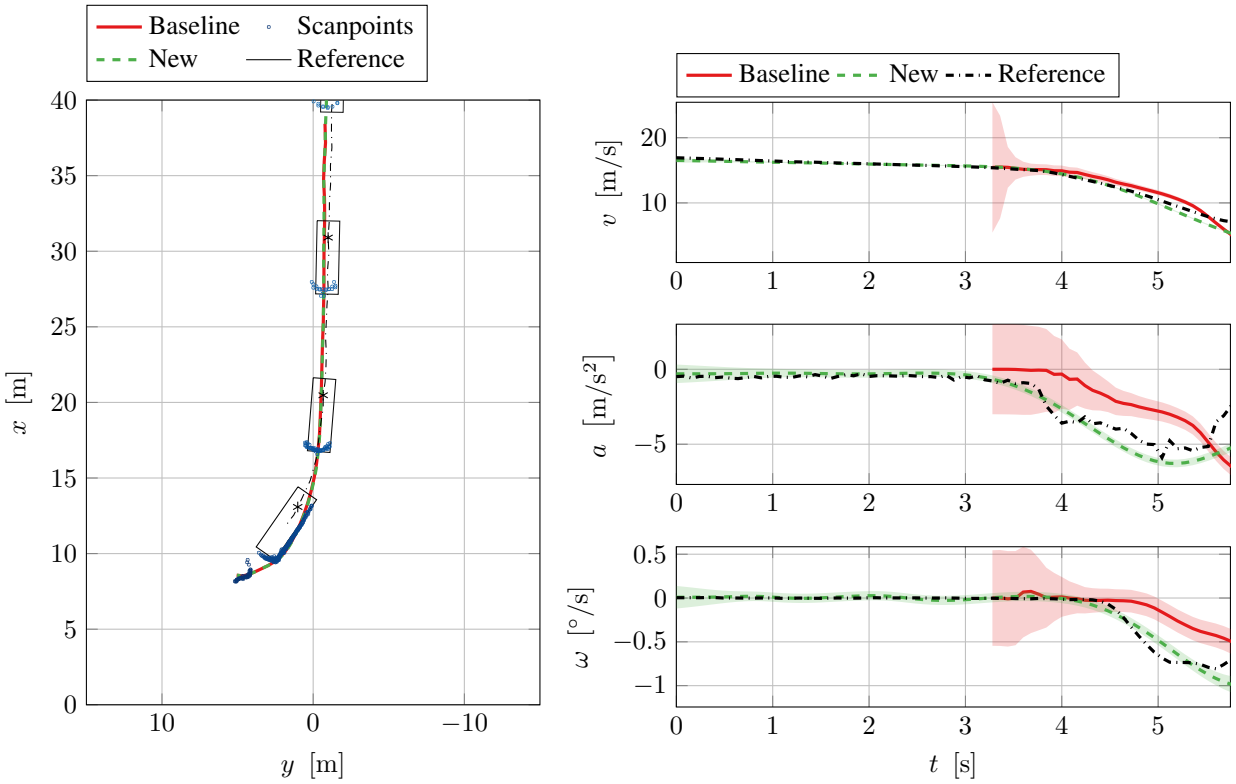

(a) Trajectory.

(b) Motion state variables.

Fig. 8: The target vehicle approaches the ego-vehicle in a left turn across manoeuvre. The ego-vehicle remains stationary at the origin in a. Here, the laser scanner measurements (blue) and trajectory estimates (red, green) are visualised (for visual clarity, only every 10th cycle is shown). Ground truth positions are illustrated in black. Estimates of velocity, acceleration and yaw rate are shown in b with their estimated covariance as indicated by the shaded $\pm 1\sigma$ intervals. Observe that even the smoothed estimates become inconsistent during the vehicle's turning phase. This can be attributed to pseudo motion that is induced by a shift of the point cloud centroid.

of highly automated vehicles, e.g. by enabling data-driven simulation environments. As has been shown in this work, already a few principled post processing techniques can increase the accuracy remarkably, which will benefit said applications.

It is beyond the scope of this work to contribute to more but a few elementary parts of laser scanner signal processing. The following aspects could provide opportunities for further fruitful research. First, this work employed an EKS under a Gaussian noise assumption for state estimation. When extended to more general noise models, i.e. including outliers, the estimator's robustness could be improved [22]. Second, one could retrieve further information from the raw scan point clouds and integrate them into the state estimator. One possibility are the translation and rotation estimates given by the WICP algorithm [7]. Lastly, the inference of semantic object class labels would certainly benefit from post processing. This task is in general challenging since scan points are often sparse but could be remedied by backward propagation of information.

References

[1] J. E. Stellet, M. R. Zofka, J. Schumacher, T. Schamm, F. Niewels, and J. M. Zöllner, "Testing of advanced driver assistance towards automated driving: A survey and taxonomy on existing approaches and open questions," in *Intelligent Transportation Systems (ITSC), 18th IEEE International Conference on*, 2015, pp. 1455–1462.

[2] U. Lages, M. Spencer, and R. Katz, "Automatic scenario generation based on laserscanner reference data and advanced offline processing," in *Intelligent Vehicles Symposium (IV), IEEE*, 2013, pp. 153–155.

[3] M. Zofka, F. Kuhnt, R. Kohlhaas, C. Rist, T. Schamm, and J. Zöllner, "Data-driven simulation and parametrization of traffic scenarios for the development of advanced driver assistance systems," in *Information Fusion (FUSION), 18th International Conference on*, 2015, pp. 1422–1428.

[4] D. Pfeiffer, S. Morales, A. Barth, and U. Franke, "Ground truth evaluation of the stixel representation using laser scanners." in *Intelligent Transportation Systems (ITSC), 13th IEEE International Conference on*, 2010, pp. 1091–1097.

[5] F. de Ponte Müller, L. M. Navajas, and T. Strang, "Characterization of a laser scanner sensor for the use as a reference system in vehicular relative positioning," in *Communication Technologies for Vehicles*, ser. Lecture Notes in Computer Science, Springer Berlin Heidelberg, 2013, vol. 7865, pp. 146–158.

[6] N. Kämpchen, "Feature-level fusion of laser scanner and video data for advanced driver assistance systems," Ph.D. dissertation, Ulm University, 2007.

[7] A. Kapp, "Ein Beitrag zur Verbesserung und Erweiterung der Lidar-Signalverarbeitung für Fahrzeuge," Ph.D. dissertation, Universität Karlsruhe (TH), 2007.

[8] D. Z. Wang, I. Posner, and P. Newman, "Model-free detection and tracking of dynamic objects with 2D lidar," *The International Journal of Robotics Research (IJRR)*, vol. 34, no. 7, pp. 1039–1063, 2015.

[9] G. Pulford, "Taxonomy of multiple target tracking methods," *Radar, Sonar and Navigation, IEEE Proceedings*, vol. 152, no. 5, pp. 291–304, 2005.

[10] F. Gustafsson and G. Hendeby, "Some relations between extended and unscented kalman filters," *Signal Processing, IEEE Transactions on*, vol. 60, no. 2, pp. 545–555, 2012.

[11] Y. Bar-Shalom, X. R. Li, and T. Kirubarajan, *Estimation with applications to tracking and navigation*, ser. A Wiley-Interscience publication. New York: Wiley, 2001.

[12] S. Pietzsch, "Modellgestützte Sensordatenfusion von Laserscanner und Radar zur Erfassung komplexer Fahrzeugumgebungen," Dissertation, Technische Universität München, München, 2015.

[13] R. Schubert, E. Richter, and G. Wanielik, "Comparison and evaluation of advanced motion models for vehicle tracking," in *Information Fusion (FUSION), 11th International Conference on*, 2008, pp. 1–6.

[14] S. Särkkä, *Bayesian filtering and smoothing*. Cambridge University Press, 2013.

[15] W. Koch, "Fixed-interval retrodiction approach to Bayesian IMM-MHT for maneuvering multiple targets," *Aerospace and Electronic Systems, IEEE Transactions on*, vol. 36, no. 1, pp. 2–14, 2000.

[16] X. Shen, "Efficient L-shape fitting of laser scanner data for vehicle pose estimation," *Cybernetics and Intelligent Systems (CIS) and IEEE Conference on Robotics, Automation and Mechatronics (RAM), 7th IEEE International Conference on*, 2015, 173-178.

[17] H. Krim, *Statistics and analysis of shapes*. Boston Basel: Birkhäuser, 2006.

[18] A. Gelb, Ed., *Applied optimal estimation*. Cambridge, Mass.: M.I.T. Press, 1974.

[19] A. H. Jazwinski, *Stochastic processes and filtering theory*, 1970.

[20] M. Brahmi, "Reference systems for environmental perception," in Automotive Systems Engineering, Springer Berlin Heidelberg, 2013, pp. 205–221.

[21] R. Schubert, H. Klöden, G. Wanielik, and S. Kälberer, "Performance evaluation of multiple target tracking in the absence of reference data," in *Information Fusion (FUSION), 13th International Conference on*, 2010, pp. 1–7.

[22] G. Agamennoni, S. Worrall, J. Ward, and E. Nebot, "Robust nonlinear smoothing for vehicle state estimation," in *Intelligent Vehicles Symposium (IV), IEEE*, 2013, pp. 156–162.